IEEE Transactions on Vehicular Technology, Available online 26 October 2022
DOI:10.1109/TVT.2022.3217354

Cooperative Ecological Adaptive Cruise Control for Plug-in Hybrid Electric Vehicle Based on Approximate Dynamic Programming

Jie Li, Yonggang Liu, *Senior Member, IEEE*, Abbas Fotouhi, *Senior Member, IEEE*, Xiangyu Wang, Zheng Chen, *Senior Member, IEEE*, Yuanjian Zhang, *Member, IEEE*, Liang Li, *Senior Member, IEEE*

***Abstract*—Eco-driving control generates significant energy-saving potential in car-following scenarios. However, the influence of preceding vehicle may impose unnecessary velocity waves and deteriorate fuel economy. In this research, a learning-based method is exploited to achieve satisfied fuel economy for connected plug-in hybrid electric vehicles (PHEVs) with the advantage of vehicle-to-vehicle communication system. A data-driven energy consumption model is leveraged to generate reinforcement signals for approximate dynamic programming (ADP) with the consideration of nonlinear efficiency characteristics of hybrid powertrain system. An advanced ADP scheme is designed for connected PHEVs driving in car-following scenarios. Additionally, the cooperative information is incorporated to further improve the fuel economy of the vehicle under the premise of driving safety. The proposed method is mode-free and showcases acceptable computational efficiency as well as adaptability. The simulation results demonstrate that the fuel economy during car-following processes is remarkably improved through cooperative driving information, thereby partially paving the theoretical basis for energy-saving transportation.**

***Index Terms*—Eco-driving, cooperative adaptive cruise control, velocity optimization, approximate dynamic programming, plug-in hybrid electric vehicle**

I. Introduction

Energy-saving of transportation has been an important issue due to the concern of energy crisis and environmental pollution. In past decades, electrified vehicles have been progressively developed to alleviate the dependence on fuel consumption [1]. Thereinto, electric vehicles (EVs), hybrid electric vehicles (HEVs) and plug-in hybrid electric vehicles (PHEVs) have been widely investigated to promote energy consumption economy [2, 3], wherein efficient powertrain topology and energy management strategy design dominates the research focus [4-6], and have gained wide breakthrough. However, unreasonable driving styles and complicated driving environments hinder further energy-saving promotion in practical applications. While, the flourishment of connected and automated technologies raises unprecedented opportunities for energy consumption economy improvement in the transport sector. Given the chances of accessing into surrounding driving conditions, connected and automated vehicles (CAVs) are enabled to adaptively adjust the vehicle speed for further energy consumption optimization, and this is also referred to as eco-driving [7]. Nowadays, CAVs are gradually paying more and more attention to the vehicle's energy consumption with the premise of driving safety and comfort [8].

Eco-driving control mainly aims at planning velocity trajectories to reduce energy consumption, and has attracted much research attention [9, 10]. The studies of eco-driving control can be divided into three categories based on different driving scenarios, i.e., single-vehicle, car-following and multi-vehicle [11]. The eco-driving control in single-vehicle scenarios is widely investigated in recent years, and is mainly concerned about reference velocity trajectory generation or free-flow driving. Pulse and glide strategies are normally recognized as a classical eco-driving method for vehicles equipped with internal combustion engine (ICE) [12]. This scheme typically adjusts engine operating points through intermittent acceleration operations. In addition, optimization algorithms are also exploited in velocity optimization. In [13], a time-varying step-size discrete dynamic programming (DP) is presented to optimize vehicle speed more efficiently. In [14], Pontryagin's minimum principle (PMP) is employed to generate ecological driving speed in a cruise condition. In [15], a data-driven based eco-driving control strategy is illustrated to achieve co-optimization of velocity in a high computational efficiency way. Recently, machine learning methods are leveraged to realize model-free control of eco-driving. In [16], a hybrid deep reinforcement learning-based eco-driving control approach is proposed to perform appropriate longitudinal trajectories and lane-changing operations, and simulation

This work was funded by the National Natural Science Foundation of China (No. 52172400). Any opinions expressed in this paper solely belong to the authors and do not represent those of the sponsors. (Corresponding authors: Yonggang Liu, Zheng Chen).

J. Li and Y. Liu are with State Key Laboratory of Mechanical Transmission & College of Mechanical and Vehicle Engineering, Chongqing University, Chongqing, 400044, China (email: lijiecqu2015@163.com and andyliuyg@cqu.edu.cn).

Abbas Fotouhi is with Advanced Vehicle Engineering Centre, School of Aerospace, Transport and Manufacturing, Cranfield University, Cranfield, Bedfordshire, MK43 0AL, U K (e-mail: a.fotouhi@cranfield.ac.uk).

Xiangyu Wang and Liang Li are with State Key Laboratory of Automotive Safety and Energy, Tsinghua University, Beijing 100084, China (e-mail: wanxy_15@tsinghua.edu.cn and liangl@tsinghua.edu.cn).

Zheng Chen is with Faculty of Transportation Engineering, Kunming University of Science and Technology, Kunming 650500, China (e-mail: chen@kust.edu.cn).

Yuanjian Zhang is with Department of Aeronautical and Automotive Engineering, Loughborough University, Leicestershire, LE11 3TU, UK (e-mail: sagazyj@gmail.com).

results highlight that the fuel consumption is remarkably reduced by up to 46%. Furthermore, some studies also plan velocity trajectories by considering traffic lights to avoid unnecessary start/stops [17]. A hierarchical optimization framework is proposed by considering the uncertainty and dynamic variation of waiting queue and is declared to decrease the fuel consumption by 4% [18]. As previously mentioned, the eco-driving control in single-vehicle scenarios mainly plans trajectories according to speed limits, terrains and traffic lights. However, preceding vehicles are typically ignored in those researches, and eco-driving control in single-vehicle scenarios is more feasible for reference velocity planning in free traffic flow. From this point of view, eco-driving control in car-following scenarios is necessary to ensure preferable driving safety, driving comfort and fuel economy, especially when the vehicle drives in congested urban road conditions.

Adaptive cruise control (ACC) system attempts to automatically adjust the driving speed of host vehicle to maintain a safe inter-vehicle distance to preceding vehicles [19]. To further improve fuel economy, economic adaptive cruise control (Eco-ACC) becomes a promising research focus, which concentrates on optimizing fuel economy and driving safety simultaneously [20]. Most studies tend to realize Eco-ACC through model predictive control (MPC) and optimize driving speed profiles according to the dynamic movement of the preceding vehicle. In [21], a novel MPC method is proposed to optimize velocity and engine power for PHEV, and reduces the fuel consumption in a vehicle following mode. For EVs, a hierarchical control architecture based on MPC is designed to improve the operation efficiency of EVs, and the motor torque is optimized considering different modes in real time [22]. However, most optimization-based Eco-ACC strategies, to the authors' knowledge, are mainly designed based on deterministic models. These methods treat eco-driving control as an optimal control problem (OCP) and establish nonlinear numerical models of vehicle energy consumption, making it difficult to directly solve the OCP in real-time [23]. Besides, the performance of Eco-ACC strongly relies on the prediction accuracy of the preceding vehicle's motion. As introduced in [24, 25], the motion prediction error is intractable to eliminate. In addition, learning-based method, such as reinforcement learning (RL) has attracted much attention due to its generalization ability and autonomous optimal solution search capability. In [26, 27], Eco-ACC is investigated based on approximate dynamic programming (ADP) and RL with the superior performance in promoting fuel economy and robustness. In [28], a deep deterministic policy gradient-based algorithm is presented for electric CAVs in car-following scenarios to restrain unnecessary velocity fluctuations. Despite the preferable performance of RL and ADP, it is still troublesome to fully dampen unnecessary velocity fluctuations, and the fuel economy deserves further improvement. The reason is that the host vehicle in the above-mentioned studies passively follows the preceding vehicle based on only the information from radars or sensors, making its speed easily affected by the velocity variations of the preceding vehicle [29].

With the development of communication technologies, CAVs can share information through vehicle-to-vehicle (V2V) communication to coordinate movements of neighbor vehicles, which provides more possibilities to improve the performance of Eco-ACC. In the following illustrations, the sharing information between CAVs to coordinate movements is defined as cooperative information. Recently, cooperative ACC (CACC) has gained gradual attraction due to the application of coordination motion in car-following scenarios. In [30], a multiple-predecessor following strategy is employed, and the results explicitly certify the benefits of V2V communication on reducing time headway for CAVs. In [31], a CACC method based on nonlinear MPC is presented for electric CAVs to improve performance in terms of following stability and fuel economy. Moreover, in some other studies [32, 33], the influence of different factors on the stability of CACC, such as communication delays, is systematically analyzed. Despite substantial potential benefits, few studies investigate the energy-saving of CACC [34]. In other words, existing studies typically focus on driving safety and string stability in CACC, whereas the fuel economy is neglected.

Based on the above discussions, researches on ecological CACC for PHEVs are relatively few and some gaps deserve to be bridged. Firstly, most of the existing optimization-based methods have to establish accurate motion prediction and energy consumption models, making Eco-ACC for PHEVs suffer from huge computational burden and online implementation difficulty [35, 36]. The energy consumption model of PHEVs needs to include nonlinear powertrain characteristics, and the real-time direct solving of optimal eco-driving control is difficult to attain [37]. Secondly, the velocity of host vehicle is significantly affected by the motion of preceding vehicle, which constraints the fuel economy promotion [34, 38]. Most Eco-ACC methods rely on prediction algorithms to obtain the motion of the preceding vehicle while imposing an adverse impact on the performance and accuracy [39], while the cooperative information obtained via V2V communication is typically employed to strengthen string stability instead of fuel economy [40]. To fill those research gaps, this study presents an ADP-based Eco-ACC method for connected autonomous PHEVs, so as to further optimize the velocity trajectory and fuel economy in car-following scenarios. The framework of the proposed scheme is shown in Fig. 1, where the ADP algorithm is leveraged to construct a car-following control model with an actor-critic structure. This controller operates in a learning-based way without explicit numerical modeling. To integrate the nonlinear characteristics of hybrid powertrain, a data-driven energy consumption model is employed to generate reinforcement signals, which can estimate the optimal energy consumption of hybrid powertrain systems. Additionally, the cooperative information is obtained through V2V communication. Finally, an ecological CACC method is designed to combine the cooperative information and ADP-based controller, which can remarkably improve the fuel economy.

The main contributions of this research are summarized as follows: 1) a cooperative ACC method is innovatively proposed for connected and automated PHEVs with the advantage of

V2V communication to significantly improve fuel economy in car-following scenarios; 2) a learning-based controller is designed based on the ADP algorithm and data-driven energy consumption model, which can sufficiently integrate the nonlinear characteristics of hybrid powertrain systems with efficient computational capacity; and 3) the cooperative information from V2V communication is exploited to update the inputs of learning-based controller, enabling that the host vehicle can reach the anticipation of preceding vehicle motion and dampen unnecessary speed fluctuations.

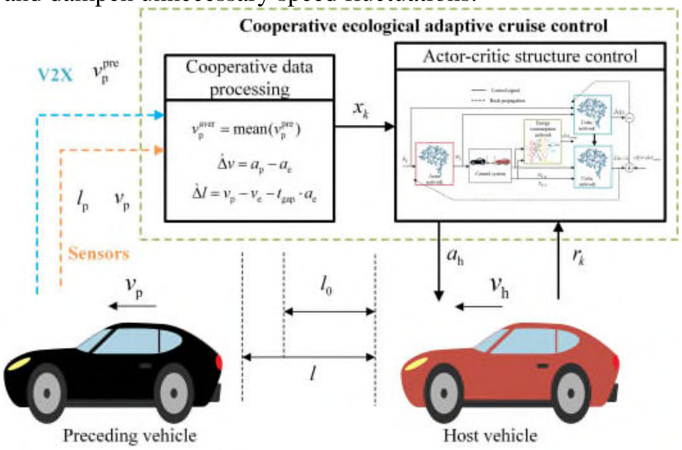

Fig. 1. The framework of the proposed cooperative adaptive cruise control approach.

The remainder of this paper is structured as follows: Section II formulates the mathematical models and optimal control problem for eco-driving in car-following scenarios. In Section III, the cooperative adaptive cruise control approach is illustrated. Section IV conducts the simulation to demonstrate the performance of the proposed method. Section V summarizes main conclusions and discusses future study.

II. Modeling of Systems

To design and demonstrate the ecological CACC approach in car-following scenarios, the longitudinal dynamics models, as well as powertrain system models, are established, and the OCP of eco-driving is formulated.

A. Longitudinal Dynamics Modeling

The longitudinal dynamics model of the CACC system consists of the dynamics model of the host vehicle and car-following system. In this research, the influence of lateral dynamics is neglected. For the host vehicle, the longitudinal dynamics model [41] is presented, as:

$$F_v = \frac{1}{3600\eta_t}\left(Mgf\cos(\alpha) + \frac{\rho_{air} C_D A v^2}{2} + Mg\sin(\alpha) + \delta M\frac{dv}{dt} \right) \tag{1}$$

where F_v is the required driving force, M is the vehicle mass, f means the rolling resistance coefficient, g is the acceleration of gravity, α expresses the road grade, C_D denotes the air drag coefficient, A indicates the frontal area of the vehicle, ρ_{air} is the air density, v is the vehicle speed, δ is the correction coefficient of rotating mass, and η_t is the transmission system efficiency. For the car-following system shown in Fig. 1, the state variables are defined, including inter-vehicle distance deviation Δl and relative velocity deviation Δv, as:

$$\Delta l = l_{\rm p} - l_{\rm h} - l_{\rm des} \tag{2}$$

$$\Delta v = v_{\rm p} - v_{\rm h} \tag{3}$$

where $l_{\rm p}$ and $l_{\rm h}$ denote the position of the preceding vehicle and the host vehicle, $v_{\rm p}$ and $v_{\rm h}$ indicate the velocity of the preceding vehicle and the host vehicle, and $l_{\rm des}$ represents the desired inter-vehicle distance. In this research, the constant time headway policy, which is a safe and classical method used in ACC controllers, is exploited to calculate the desired inter-vehicle space. Therefore, the desired inter-vehicle distance is calculated, as:

$$l_{\rm des} = t_{\rm gap} v_{\rm h} + l_0 \tag{4}$$

where $t_{\rm gap}$ is the nominal time headway, and l_0 means the standstill distance. It can be found that the desired inter-vehicle distance varies with the velocity of the host vehicle. For instance, a longer desired inter-vehicle distance is required at a higher velocity, to ensure driving safety in car-following scenarios. To guarantee driving safety, the inter-vehicle distance $d_{\rm veh}$ should keep within the safe range [42]. The limits of inter-vehicle distance can be calculated, as:

$$\begin{cases} \Delta l_{\max} = 2 + 0.5\cdot v + 0.0625\cdot v^2 \\ \Delta l_{\min} = 10 + v + 0.0825\cdot v^2 \end{cases} \tag{5}$$

where $\Delta l_{\max}$ and $\Delta l_{\min}$ are the maximum and minimum inter-vehicle distance, respectively. The dynamics models of state variables Δl and Δv are formulated as follow:

$$\dot{\Delta v} = a_{\rm p} - a_{\rm h} \tag{6}$$

$$\dot{\Delta l} = v_{\rm p} - v_{\rm h} - t_{\rm gap}\cdot a_{\rm h} \tag{7}$$

where $a_{\rm p}$ and $a_{\rm h}$ are the acceleration of the preceding vehicle and the host vehicle, respectively.

B. Powertrain System Modeling

The powertrain configuration of the studied PHEV is shown in Fig. 2. As can be found, the vehicle can be propelled individually by either the engine or the integrated starter generator (ISG), and the dual clutch transmission (DCT) is coupled with the main reducer and the motor axle to adjust their torque and speed ratios.

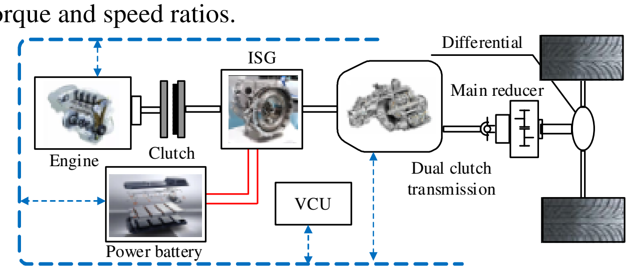

Fig. 2. Powertrain system of the PHEV.

The modeling of the studied PHEV mainly includes three parts: engine, ISG motor and power battery, and additionally the accessory power is neglected for simplification in this research. It should be note that the proposed method is mode-free, and the powertrain models constructed in this section are used for simulation. The fuel consumption rate $\dot{m}_{fuel}$ (unit: g/kwh) is calculated by interpolating torque T_e and speed n_e, as:

$$\dot{m}_{fuel} = f_{\mathrm{e}}(T_e, n_e) \tag{8}$$

where f_{e} denotes the nonlinear map acquired by calibration experiments. Thus, the total fuel consumption Q_{fuel} (unit: L) can be formulated as:

$$Q_{fuel} = \int \frac{\dot{m}_{fuel} \cdot T_e \cdot n_e}{3.6 \times 10^6 \times 9500 \rho} dt \tag{9}$$

where ρ is the density of gasoline. Similarly, the efficiency model of ISG is acquired by experimental data, and an interpolation model is constructed to describe the relationship among efficiency η_m, motor torque T_m and motor speed n_m, as:

$$\eta_m = f_m(T_m, n_m) \tag{10}$$

where f_m denotes the efficiency map of ISG. The battery power P_b can be formulated as:

$$P_b = \frac{T_m \cdot n_m}{9550 \eta_m} \tag{11}$$

An open circuit voltage source (OCV)- resistance model is adopted to characterize the battery's electrical performance. Based on the Kichoff's law, the battery current can be calculated, as:

$$I_b = \frac{E - \sqrt{E^2 - 4RP_b}}{2R} \tag{12}$$

$$SOC(t) = SOC_0 - \frac{\int_0^t I_b(t) dt}{Q_b} \tag{13}$$

where SOC_0 is the initial SOC, Q_b is the battery capacity, I_b is the battery current, E and R represent the open circuit voltage and the battery internal resistance, which can be acquired by interpolation. The electricity consumption Q_{ele} can be accumulated, as:

$$Q_{ele} = \int \frac{I_{\mathrm{b}} \cdot E}{3.600 \times 10^6} dt \tag{14}$$

C. Control Problem Formulation

The control objective in this study is to minimize the fuel consumption of the host vehicle with the inter-vehicle distance in a safe range. The inter-vehicle distance deviation and relative velocity deviation are chosen to calculate the dynamic performance index. Furthermore, the energy consumption cost $cost_{energy}$ is defined as the fuel economy index for PHEVs. As a result, the objective function of Eco-ACC can be formulated as:

$$J = \int_0^T (\lambda_1 \Delta v^2 + \lambda_2 \Delta l^2 + \lambda_3 \cos t_{energy}) dt \tag{15}$$

where λ_1, λ_2 and λ_3 represent the weight factors of dynamic performance index and fuel economy index, and T is the travel time for the whole car-following scenario. To reduce energy consumption cost through longitudinal dynamics control, the acceleration is defined as the control variable. In the OCP of Eco-ACC for PHEVs, there are four state variables to describe the system state, including the host vehicle's velocity, SOC, inter-vehicle distance deviation and relative velocity deviation. Besides, the following constraints should be imposed, as:

$$\begin{cases} a_{\min} \le a_{\mathrm{h}} \le a_{\max} \\ v_{\min} \le v_{\mathrm{h}} \le v_{\max} \\ SOC_{min} \le SOC \le SOC_{max} \\ \Delta v_{\min} \le \Delta v \le \Delta v_{\max} \\ \Delta l_{\min} \le \Delta l \le \Delta l_{\max} \end{cases} \tag{16}$$

Obviously, common optimization solutions suffer from huge difficulty in directly solving the OCP due to the complex state variables. To tackle this problem, ADP is exploited to construct a model-free control method, which can adaptively search optimal control decisions without establishing explicit numerical models

III. Cooperative Ecological Adaptive Control Based on ADP

The proposed CACC approach is elaborated and shown in Fig. 3. The ADP approach is pre-trained offline with different driving cycles to obtain an acceptable controller. During training, the reinforcement signal evaluates the instantons cost and returned back to the critic network and the action network for the controller update. Moreover, the V2V communication and sensors transfer the cooperative information to the car-following controller, which generates the optimal decisions and updates parameters according to the system state and instantaneous cost reward. Ultimately, the ecological velocity trajectories are generated to improve fuel economy.

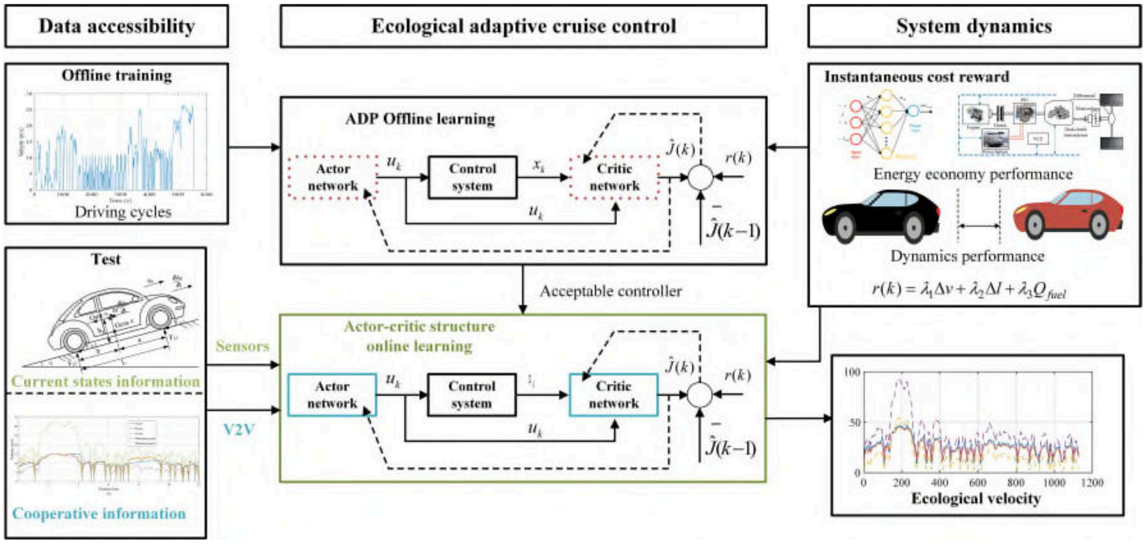

Fig. 3. Cooperative adaptive cruise control approach based on approximate dynamic programming.

A. Approximate Dynamic Programming

For the eco-driving control of PHEVs, it is difficult to directly solve the OCP due to the presence of nonlinear systems, such as the energy consumption model. Hence, the multiple state variables and control decisions make OCP of eco-driving on PHEVs suffer from the curse of dimensionality, and normal optimization algorithms are failed to search for optimal control decisions online. The RL algorithm has gained great attention in recent years, and it is verified efficient in solving complex nonlinear OCP. The ADP algorithm is a branch of RL, which combines the theory of RL and Bellman optimality [43]. In this method, the value function and optimal control policy are replaced via neural networks which make the controller is model-free and do not have to construct explicit models for optimal control. Based on the actor-critic structure, the ADP algorithm can adaptively learn how to make optimal decisions via continuous trial-and-error interactions with the environment. On this account, the ADP algorithm is leveraged to establish the proposed controller, and the Eco-ACC is treated as a nonlinear discrete-time system. Based on Bellman optimality, the value function can be calculated as:

$$J(x_N)=\sum_{k=N}^{\infty}L(x_{k+1},u_{k+1})+L(x_N) \tag{17}$$

where $L(x_k,u_k)$ indicates the cost value at each step. Furthermore, a discount factor β, which varies in the range of 0 to 1, is added to the value function. The discount factor can adjust the impact effect of future cost according to the current value function, which is formulated as:

$$J(x_N)=L(x_N)+\beta J(x_{N+1}) \tag{18}$$

Thus, the target of optimization is to find an optimal control policy u_k^* to minimize then value function according to the instantaneous system state, as:

$$u_N^*=\arg\min\left\{L(x_N,u_N)+J^*(x_{N+1})\right\} \tag{19}$$

The optimal value function can be expressed as:

$$J^*(x_N)=L(x_N,u_N^*)+\beta J^*(x_{N+1}) \tag{20}$$

It can be found that there are two crucial sections in Bellman optimality, i.e., optimal value function $J^*(x_N)$ and optimal control policy u_N^*. For traditional DP, the optimal value function cannot be directly obtained in advance. Therefore, a backward recursive calculation is indispensable to obtain the optimal value function, which extremely increases the computational burden. On the other hand, the ADP algorithm normally replaces these two components via critic network and actor network. The constructed actor-critic structure can continuously learn the optimal control policy and value function to solve the OCP in a forward manner. An actor-critic ADP structure exploited in this study is shown in Fig. 4. This structure consists of a critic network and an actor network. The reinforcement signal, referred to as instantaneous cost in the control field, will be employed to calculate the error of the critic network, and the error will be returned back to improve the accuracy of the critic network. Similarly, the outputs of the critic network will be rewarded to the actor network for learning. Unlike ICE vehicles or EVs, the energy consumption of PHEV cannot be directly calculated according to velocity and acceleration due to the existence of two energy sources in hybrid powertrain system. Most of existing researches promote fuel economy of PHEV via smoothing velocity and restraining acceleration, and the nonlinear characteristics of powertrain system are not included in the controller [37]. Obviously, calculating reinforcement signal according to energy consumption can further promote fuel economy. In our previous work [15], a data-driven energy consumption cost model is established to approximate the optimal energy consumption cost considering the nonlinear characteristics of the hybrid powertrain. Unlike the common ACC methods based on ADP, the data-driven energy consumption model is applied to generate the reinforcement signal during the offline training of the critic-actor controller. By this manner, the powertrain characteristics are integrated into the actor-critic controller.

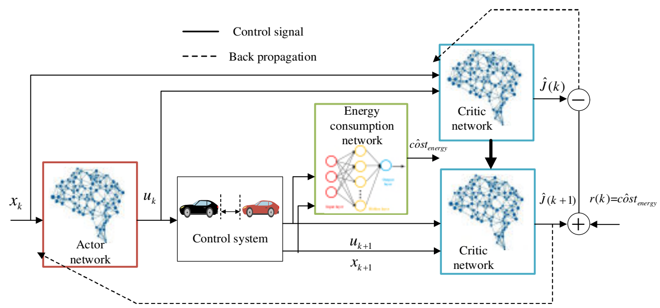

Fig. 4. The proposed actor-critic structure.

B. Ecological Adaptive Cruise Control Based on ADP

To design the ecological adaptive cruise control approach based on ADP, the state variables, control variables, critic network and actor network need be defined to instruct the controller design. The state variable vector $\mathbf{x_k}$ is defined as $[\Delta l, \Delta v]^{\mathrm{T}}$, and the control variable $\mathbf{u_k}$ is selected as a_{h}. As introduced above, the data-driven energy consumption model will generate estimated energy consumption cost to calculate the reinforcement signal.

For the critic network, this module is employed to approximate the optimal value function. The structure of the critic network should be simplified with the premise of fulfilling estimation performance so as to promote calculation efficiency. In this research, an artificial network with a hidden layer is used to construct the critic network. The inputs of the critic network consist of a state variable vector and a control variable vector. The Sigmoid transfer function is applied in the hidden layer, and the Purelin transfer function is employed for the output layer [27]. The output is the estimated optimal cost value from step k to the end, as:

$$\hat{J}(x_k, u_k) = f_{\mathrm{critic}}(x_k, u_k) \tag{21}$$

where f_{critic} denotes the nonlinear map function describing the relationship between the inputs and the optimal cost value. With the network constructed, a naive weight vector will be assigned to the critic network. Furthermore, the weight vector will be updated through repetitive interactions with the environment. Based on the analysis above, the error function of the critic network in each step can be defined as:

$$e_{\mathrm{c}}(k) = \hat{J}(k) - r(k) - \beta \hat{J}(k+1) \tag{22}$$

$$r(k) = \lambda_1 \Delta v^2 + \lambda_2 \Delta l^2 + \lambda_3 \hat{c}ost_{energy} \tag{23}$$

$$\hat{c}ost_{energy} = f_{NNC}(x_k, u_k) \tag{24}$$

where $r(k)$ is reinforcement signal, which is comprised of fuel economy index and dynamics performance index, $\hat{c}ost_{energy}$ is the estimated energy consumption cost generated by the data-driven energy consumption model, and f_{NNC} represents the data-driven energy consumption model, of which the detailed construction can be found in our previous study [15]. From eq. (22), it can be observed that reinforcement signal can integrate fuel economy index and dynamics performance index into the approximated value function through trail-and-error. The target of learning is to minimize the output error of the critic network via updating the weight vector, so that it enables the critic network to approximate the optimal value function. Therefore, the objective function for the critic network learning is presented as:

$$E_{\mathrm{c}}(k) = \frac{1}{2} e_{\mathrm{c}}^{\,2}(k) \tag{25}$$

To update the weight vector of the critic network, the gradient descent adaptation algorithm is leveraged to iteratively update weights. The formulations of the critic network updating in each step are expressed as:

$$\begin{cases} \mathbf{w}_{\mathrm{c}}(k+1) = \mathbf{w}_{\mathrm{c}}(k) + \Delta \mathbf{w}_{\mathrm{c}}(k) \\ \Delta \mathbf{w}_{\mathrm{c}}(k) = \eta_{\mathrm{c}}(k)\left[-\dfrac{\partial E_{\mathrm{c}}(k)}{\partial \mathbf{w}_{\mathrm{c}}(k)}\right] \\ \dfrac{\partial E_{\mathrm{c}}(k)}{\partial \mathbf{w}_{\mathrm{c}}(k)} = \dfrac{\partial E_{\mathrm{c}}(k)}{\partial \hat{J}(k)} \dfrac{\partial \hat{J}(k)}{\partial \mathbf{w}_{\mathrm{c}}(k)} \end{cases} \tag{26}$$

where $\mathbf{w}_{\mathrm{c}}(k)$ is the weight vector of the critic network, $\Delta \mathbf{w}_{\mathrm{c}}(k)$ is the updated value of the critic network weight vector, η_{c} is the critic network learning rate which can be used to adjust the learning performance to avoid over-fitting.

The actor network accounts for approximating the optimal control policy, with the input of state variables and the output of estimated optimal control. Similarly, an artificial neural network with one hidden layer is harnessed to construct the actor network. The hyperbolic tangent transfer function and Purelin transfer function are applied in the hidden layer and output layer, respectively [27]. The output of the actor network can be expressed as:

$$\hat{u}^*(k) = f_{\mathrm{act}}(x_k) \tag{27}$$

where $\hat{u}^*(k)$ is the approximated optimal control policy, and f_{act} reflects the nonlinear relationship between the state variables and the optimal control decisions. The learning of the actor network is performed to generate the control decisions for minimizing the output of the critic network. To achieve this purpose, the learning objective of the actor network is expressed as:

$$E_{\mathrm{a}}(k) = \hat{J}(x_k, u_k) \tag{28}$$

To learn the optimal control policy, the gradient descent adaptation algorithm is applied to update the weight vector as follow:

$$\begin{cases} \mathbf{w}_{\mathrm{a}}(k+1) = \mathbf{w}_{\mathrm{a}}(k) + \Delta \mathbf{w}_{\mathrm{a}}(k) \\ \Delta \mathbf{w}_{\mathrm{a}}(k) = \eta_{\mathrm{a}}(k)\left[-\dfrac{\partial E_{\mathrm{a}}(k)}{\partial \mathbf{w}_{\mathrm{a}}(k)}\right] \\ \dfrac{\partial E_{\mathrm{a}}(k)}{\partial \mathbf{w}_{\mathrm{a}}(k)} = \dfrac{\partial E_{\mathrm{a}}(k)}{\partial \hat{J}(k)} \dfrac{\partial \hat{J}(k)}{\partial \hat{u}^*(k)} \dfrac{\partial \hat{u}^*(k)}{\partial \mathbf{w}_{\mathrm{a}}(k)} \end{cases} \tag{29}$$

where $\mathbf{w}_{\mathrm{a}}(k)$ is the weight vector of the actor network, $\Delta \mathbf{w}_{\mathrm{a}}(k)$ is the updated value of the actor network's weight vector, and η_{a} is the actor network learning rate, which should be reasonably adjusted to contribute to the performance of learning.

C. Cooperative Adaptive Cruise Control

As discussed before, V2V communication and automatic driving provide more opportunities for performance promotion of Eco-ACC. Traditional Eco-ACC methods typically account for the influence of preceding vehicles by speed prediction algorithm. Most current studies need to predict explicit velocity trajectories, which have drawbacks in terms of accuracy and computational efficiency [21, 22, 24]. In this research, we assume that both the preceding vehicle and the host vehicle are CAVs, indicating that these vehicles can automatically plan velocity trajectories and share cooperative information through the V2V communication.

To tackle problems of prediction-based ACC, the preceding vehicle transfers the average planned velocity $v_{\mathrm{p}}^{\mathrm{aver}}$ and the average planned acceleration $a_{\mathrm{p}}^{\mathrm{aver}}$ during a specific future horizon (referred to as cooperation horizon in this study) to the host vehicle. While traditional prediction-based ACC methods normally have to predict explicit velocity trajectories. Compared with explicit speed trajectories, the implementation of average planned velocity and average acceleration can contribute to the robustness improvement of the proposed method.

On this basis, the cooperative information, i.e., average velocity $v_{\mathrm{p}}^{\mathrm{aver}}$ and average acceleration $a_{\mathrm{p}}^{\mathrm{aver}}$ of the preceding vehicle, will be disseminated to the host vehicle by V2V communication. In addition, instantaneous information of the preceding vehicle is obtained through sensors, including position, velocity and acceleration. The proposed CACC information transmit mechanism is shown in Fig. 5. Based on the cooperative information, the velocity and acceleration of the preceding vehicle are corrected by considering the future planned motion, as:

$$a_{\mathrm{p}}^{\mathrm{c}}=\mathrm{mean}(a_{\mathrm{p}}^{\mathrm{aver}}+a_{\mathrm{p}}) \tag{30}$$

$$v_{\mathrm{p}}^{\mathrm{c}}=\mathrm{mean}(v_{\mathrm{p}}^{\mathrm{aver}}+v_{\mathrm{p}}) \tag{31}$$

According to the received cooperative information, the inputs of the ADP-based controller is regulated to correct inter-vehicle distance deviation Δl^{c} and relative velocity deviation Δv^{c}, as:

$$\Delta l^{\mathrm{c}}=l_{\mathrm{p}}^{\mathrm{c}}-l_{\mathrm{h}}-l_{\mathrm{des}} \tag{32}$$

$$\Delta v^{\mathrm{c}}=v_{\mathrm{p}}^{\mathrm{c}}-v_{\mathrm{h}} \tag{33}$$

where $l_{\mathrm{p}}^{\mathrm{c}}$ is the corrected position of the preceding vehicle. Accordingly, eqs. (6) and (7) can be reformulated a:

$$\Delta\dot{l}^{\mathrm{c}}=v_{\mathrm{p}}^{\mathrm{c}}-v_{\mathrm{h}}-t_{\mathrm{gap}}\cdot a_{\mathrm{h}} \tag{34}$$

$$\Delta\dot{v}^{\mathrm{c}}=a_{\mathrm{p}}^{\mathrm{c}}-a_{\mathrm{h}} \tag{35}$$

With the inputs modified by cooperative information, the host vehicle can acquire the future motion decision of the preceding vehicle. The average acceleration $a_{\mathrm{p}}^{\mathrm{aver}}$ indicates the future motion tendency of the preceding vehicle, while the average velocity $v_{\mathrm{p}}^{\mathrm{aver}}$ reflects the future motion magnitude of the preceding vehicle. As a result, the host vehicle can further improve the fuel economy with inter-vehicle distance within a safe range, considering the future motion of the preceding vehicle.

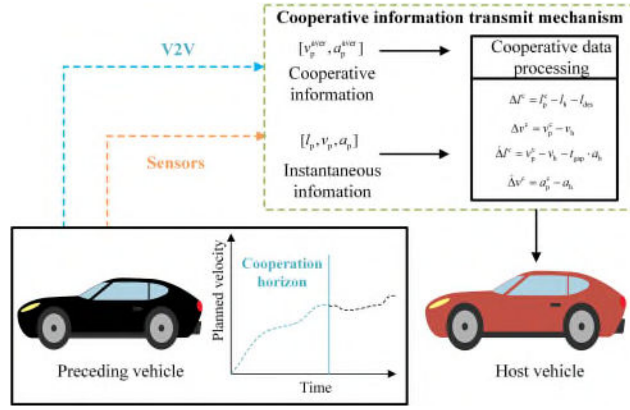

Fig. 5. Cooperative information transmit mechanism.

IV. Simulation Analysis

To verify the performance of the proposed method, simulation case studies are conducted in MATLAB environment. In the simulations, we assume that both vehicles drive at a straight road with zero road grade. The initial velocity of the host vehicle and the preceding vehicle is set as zero, and the initial inter-vehicle distance is 15 m. In addition, the influences of temperature on engine, motor and battery output are neglected in this research. To quantitively evaluate the performance improvement generated by velocity optimization, the DP algorithm is employed in different approaches to realize energy management. The proposed approach (simplified as C-EACC) is compared with two existing benchmarks: 1) a proportional-integral-derivative (PID)-based ACC approach (PID-ACC) [44], and 2) an ADP-based Eco-ACC approach (ADP-EACC) [26]. The former tracks the velocity of preceding vehicle without considering fuel economy, while the latter optimizes fuel economy of the host vehicle without the knowledge of cooperative information. The details of the two methods can be found in [44] and [26], and not elaborated in this article. The parameters of PID controller are set as: $K_p = 0.9$, $K_d = 0.213$ and $K_i = 0.1$. To quantitively evaluate the performance improvement generated by cooperative information, the parameters of the ADP-EACC method are set the same as the proposed method. The basic parameters of the host vehicle are presented in Table I. The energy consumption cost is selected to evaluate the fuel economy of PHEV where the fuel price of CNY 7.8 per liter, and the price of electricity is set as CNY 0.52 per kWh.

TABLE I
THE BASIC PARAMETERS OF PHEV

Characteristic	Value
Mass (kg)	1350
Frontal area (m^2)	2.82
Air drag coefficient	0.3146
Tire rolling radius (m)	0.308
Rolling resistance coefficient	0.0135
ISG peak power (kW)	40

Engine peak power (kW)	80
Battery capacity (Ah)	40
DCT gear ratio	3.917/2.429/1.436/1.021/0.848/0.667

The parameters setting of the ADP algorithm is performed via trial-and-error. Wherein, the number of neurons in network should be minimized to promote calculation efficiency on the premise of ensuring control performance; the learning rate of network, maximum iteration number and error tolerance can generate impact on converge speed. However, an excessive learning rate may result in non-convergence and should be avoided. The discount factor reflects the influence of future cost on value function. A higher discount factor will search optimal control decision, with more future cost taken into consideration. The outcomes of parameters setting are presented in Table II. A comprehensive driving cycle is constructed as the preceding vehicle to train the actor-critic controller offline. The convergence of objective value during offline training is shown in Fig. 6. It can be found that the objective value decreases with the increase of training epochs. The objective value gradually achieves convergence after 26 training epochs. Thus, an acceptable ADP-based control is obtained for online simulation.

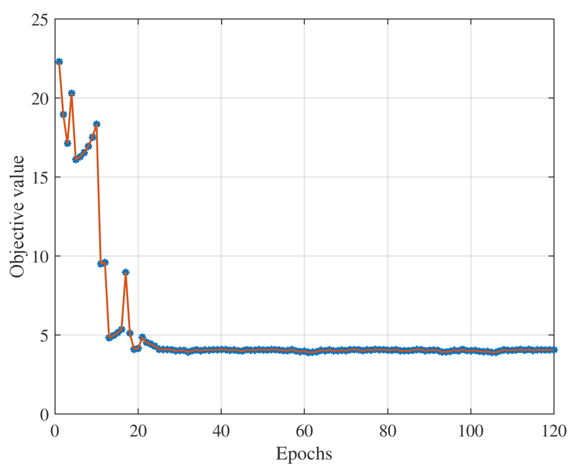

Fig. 6. Convergence curves during offline training.

During the real-time control, the energy cost, velocity deviation as well as desired inter-vehicle distance are measured and the reinforcement signal is calculated according to (23). The weighting parameters of actor network and critic network are adapted online based on the actor-critic structure described in Section III. Once the maximum iteration number or the error tolerance is reached, the online learning is stopped, and the control decision is outputted by the actor network. It should be note that the proposed control strategy is model-free.

TABLE II
THE BASIC PARAMETERS OF APPROXIMATE DYNAMIC PROGRAMMING

Parameters	Value
Number of neurons in critic network	60
Number of neurons in action network	60
Learning rate of critic network	1.00e-4
Learning rate of action network	6.00e-6
Maximum iteration number of critic network	20
Maximum iteration number of action network	20
Error tolerance of critic network	$1.00e^{-6}$
Error tolerance of action network	$1.00e^{-8}$
Discount factor	0.9
The weight of velocity deviation λ_1	0.01
The weight of desired inter-vehicle distance deviation λ_2	0.0032
The weight of energy consumption λ_3	20

A. Sensitivities to Cooperation

The region of cooperation horizon has a significant impact on the performance of the proposed C-EACC method. We firstly analyze the sensitivity of the proposed method with different cooperation horizons. Referring to the parameter setting of the common prediction-based ACC approaches [22, 42], six cooperation horizon samples are discretely chosen from 1 s to 10 s, i.e., $[1,2,3,5,8,10]$. In this test, the proposed method is compared with the PID-ACC method. The standard driving cycle UDDS, which is not included in the comprehensive driving cycle for training, is exploited as the testing cycle of the preceding vehicle. And the initial battery state of charge (SOC) of the host vehicle is set as 0.4, so that the engine can be enrolled in propulsion. The simulation results with different cooperation horizons are summarized in Table III. Compared with the PID-ACC method, it can be found that C-EACC methods with different cooperation horizons can improve fuel economy from 4.21% to utmost 9.06%. However, the constraint of inter-vehicle distance is violated when the cooperation horizon is set to 10 s and 8 s, indicating that the safety is not met in these cases.

TABLE III
SIMULATION RESULTS OF DIFFERENT COOPERATION REGIONS

Cooperation horizon	Energy consumption cost (CNY)	Average inter-vehicle distance deviation (m)	Average velocity deviation (m/s)	Meet maximum/minimum inter-vehicle distance constraints	Fuel economy improvement (%)
10s	1.51	2.22	0.89	NO	8.77
8s	1.51	1.99	0.83	NO	9.06
5s	1.52	1.62	0.72	YES	8.66
3s	1.55	1.44	0.65	YES	6.63
2s	1.57	1.42	0.61	YES	5.46
1s	1.59	1.41	0.58	YES	4.21

The simulation results demonstrate that the variation of cooperation horizon generates significant impacts on driving safety and fuel economy. The change tendency of the average inter-vehicle distance deviation is shown in Fig. 7. A decline of the average inter-vehicle distance deviation is observed with the decrease of cooperation horizon, and the change in magnitude of the average distance deviation tends to be flat when the cooperation horizon decreases to 3 s. It indicates that the driving safety is improved with cooperation horizon decline. By contrast, the fuel economy deteriorates when the cooperation horizon is decreased.

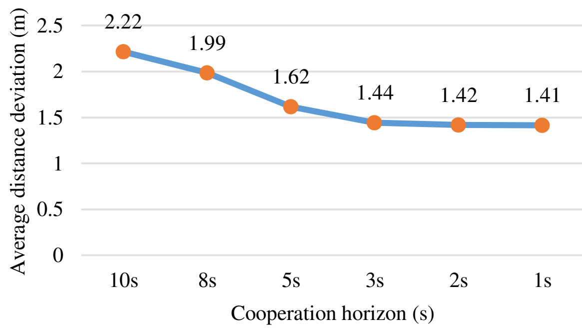

(a)

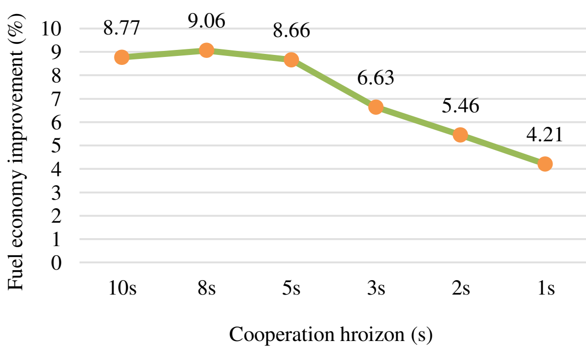

(b)

Fig. 7. Performance analysis with different cooperation horizons. (a) average inter-vehicle distance deviation, (b) fuel economy improvement.

The velocity trajectories with different cooperation horizons are shown in Fig. 8. While all test cases can follow the driving speed of the preceding vehicle on the whole, the approaches with smaller cooperation horizons show better performance in velocity tracking, as shown in Fig. 8. The reason is that a longer cooperation horizon imposes more modifications on the velocity and acceleration of the preceding vehicle, and consequently it contributes to avoiding unnecessary velocity fluctuations and reducing energy consumption. However, excessive modification on driving states of the preceding vehicle also harms driving safety. To balance the conflict between fuel economy and driving safety, the cooperation horizon is defined as 3 s in the following simulation tests based on the above-mentioned analysis.

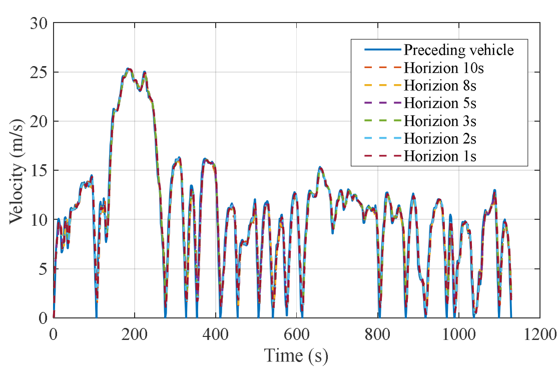

(a)

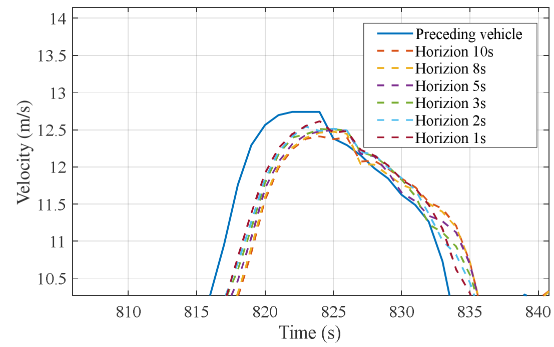

(b)

Fig. 8. Velocity trajectories with different cooperation horizons. (a) overall velocity trajectories, (b) magnification of velocity trajectories.

B. Performance Analysis

To further analyze the performance of the proposed C-EACC method, the simulation results are analyzed in terms of velocity optimization and powertrain control. The simulation parameters are the same as they were in the last test. The C-EACC method, which has a cooperation horizon of 3 s, is compared with the PID-ACC and the ADP-EACC methods. The simulations are conducted on a laptop equipped with an AMD Ryzen7 CPU. The calculation time of the C-EACC method and PID-ACC method is 26.33 s and 23.88 s, respectively, indicating that the proposed method has a tiny difference with the baseline case in computational burden.

The results of velocity optimization are shown in Fig. 9. Compared with the two benchmarks, the C-EACC method can effectively restrain velocity fluctuations due to the accessibility to the cooperative information, as shown in Fig. 9 (a). By contrast, PID-ACC and ADP-EACC only passively track the velocity of the preceding vehicle, and are incapable of avoiding unnecessary velocity fluctuations. Fig. 9 (b) illustrates the inter-vehicle distance of different methods, and we can find all three approaches can track the driving speed of the preceding vehicle, and the inter-vehicle distance is maintained within the safe range. The inter-vehicle distance deviation yielded by the proposed method is constrained within -2 m and 2 m most of the time, indicating preferable performance in car-following and driving safety. Fig. 9 (d) illustrates the acceleration decisions of the C-EACC method, and it can be found that acceleration is normally kept within small values, changing from -1.5 m/s^2 to 1.5 m/s^2 and contributing to the promotion of fuel economy and driving comfort.

The results of the powertrain system are shown in Fig. 10. Similar engine torque values are observed, since the same energy management strategy, i.e., the DP algorithm, is employed in all three methods. However, the PID-ACC method tends to frequently start/stop the engine and outputs higher engine torque, compared with the other two methods. The reason lies in that the host vehicle controlled by the PID-ACC method needs to follow more velocity waves, leading to more frequent on/off operations of the engine. The same decrease tendency of SOC trajectories is observed in all three approaches, and all of them drops to 0.3 at the end of trip. It indicates that all the three methods lead to the same electricity consumption, and the fuel efficiency can be quantitatively evaluated through the energy consumption cost. However, the PID-ACC and ADP-EACC methods show higher SOC value compared with the proposed method, due to the frequent operation of the engine.

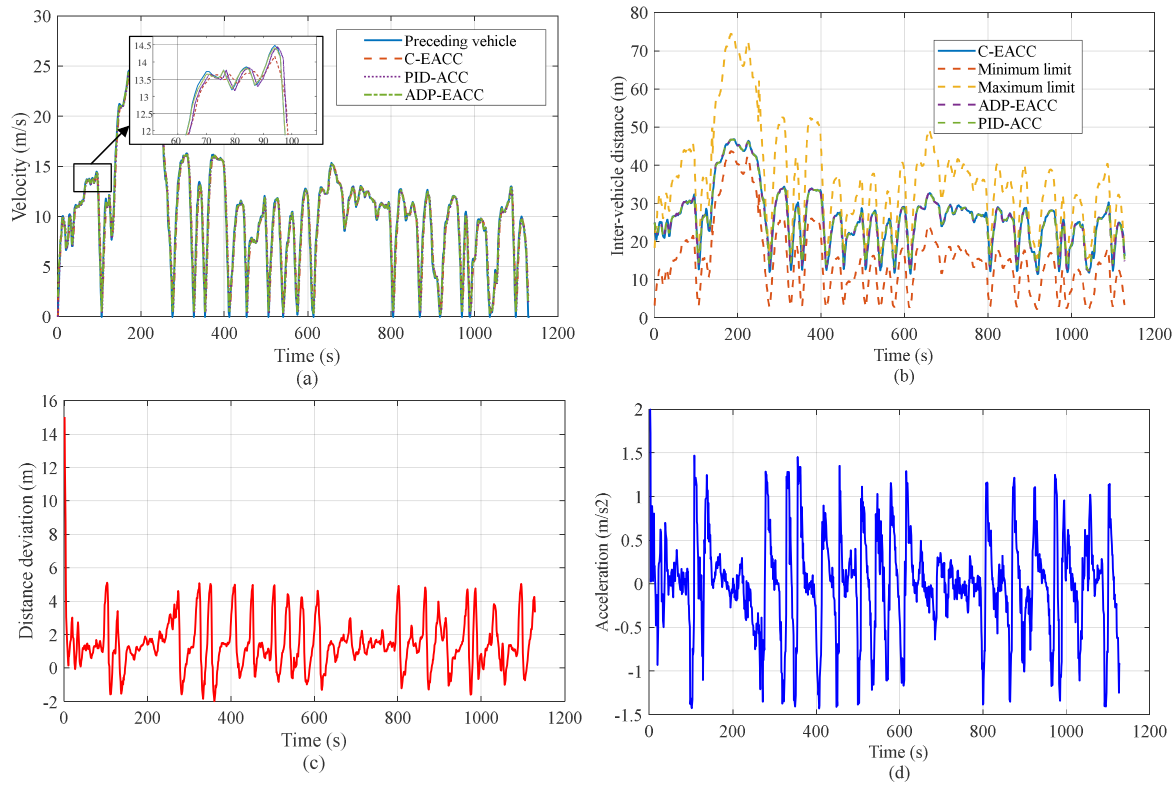

Fig. 9. Velocity optimization results of different approaches. (a) velocity trajectories, (b) inter-vehicle distance, (c) inter-vehicle distance deviation of C-EACC method, (d) longitudinal acceleration of C-EACC method.

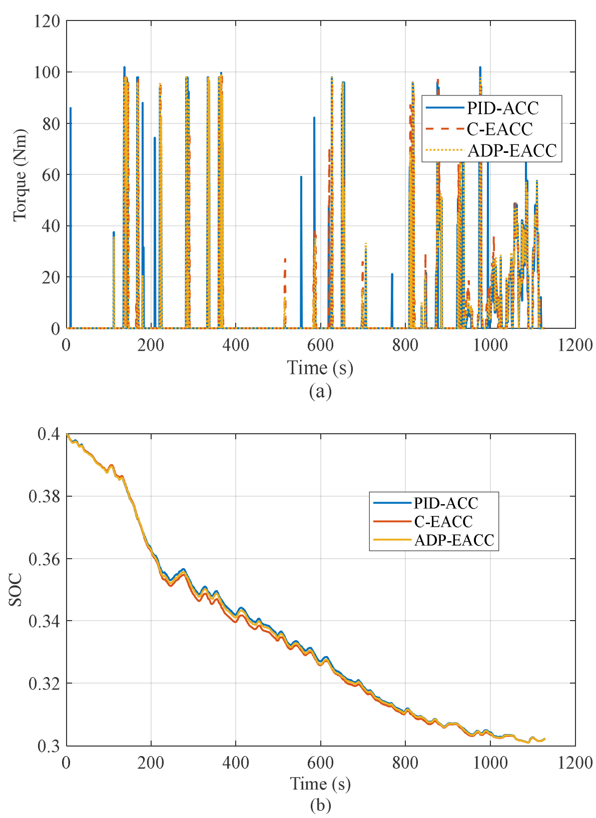

Fig. 10. Simulation results of the powertrain system. (a) engine torque, (b) SOC trajectories.

To further analyze the energy-saving performance, different initial SOC values are applied in the simulation. The fuel economy of C-EACC and ADP-EACC method are compared with the PID-ACC method, and fuel economy improvement is summarized in Table IV. Compared with the PID-ACC method, a notable improvement is raised by C-EACC at different initial SOCs, and the maximum improvement is 8.28%. By contrast, the ADP-EACC method generates a slight improvement in different initial SOC by up to 2.37%. The lowest improvement is observed when the initial SOC is 0.31 for both C-EACC and ADP-EACC methods. In summary, the proposed approach can raise notable improvements in fuel economy for PHEVs in the premise of fulfilling driving safety and driving comfort. Moreover, the cooperative information can dramatically mitigate velocity fluctuations and further reduce energy consumption, compared with the existing Eco-ACC method.

TABLE IV

FUEL ECONOMY COMPARISON OF UDDS DRIVING CYCLE

Initial SOC	C-EACC		ADP-EACC		PID-ACC
	Energy consumption cost (CNY)	Fuel economy improvement (%)	Energy consumption cost (CNY)	Fuel economy improvement (%)	Energy consumption cost (CNY)
0.5	0.85	4.49	0.88	1.12	0.89
0.4	1.55	8.28	1.65	2.37	1.69
0.35	2.63	5.05	2.74	1.08	2.77
0.31	3.66	2.66	3.75	0.27	3.76

C. Adaptability analysis

The simulation tests above are conducted in a standard driving cycle by assuming that the cooperative information is completely accurate. In this section, we firstly test the robustness of the C-EACC method with cooperative information affected by different deviations, and a real-world driving cycle is also employed to test the adaptability to different driving cycles. The PID-based model is applied to track the velocity of the preceding vehicle so as to artificially generate velocity trajectories with deviations. Thus, the velocity trajectories generated by the PID-based model is transmitted to the host vehicle as cooperative information, and the real velocity of the preceding vehicle is set as the UDDS driving cycle. The average velocity error is selected to evaluate deviations in cooperative information, as:

$$ev_{\text{ave}} = \frac{1}{N}\sum_{k=1}^{N}\left|v_{\text{real}}^{k} - v_{\text{planned}}^{k}\right| \tag{36}$$

where v_{real}^{k} is the real velocity of preceding vehicle, v_{planned}^{k} is the planned velocity of preceding vehicle in cooperative information, N is the duration of the driving cycle.

Three cases with different cooperative information deviations are considered for comparison, and the results are shown in Table V. It can be found that the deviation of cooperative information has a notable influence on fuel economy. The proposed method can reduce the energy consumption cost by 8.28% when the cooperative information is absolutely accurate. By contrast, the fuel economy improvement is decreased by 2.96% to 4.73% when deviations are imposed on cooperative information. Despite the affection of information deviation, the C-EACC method still effectively reduces energy consumption even with information deviations, where the minimum improvement is 2.96%. In addition, a declining tendency is observed in fuel economy with the increased cooperative information deviation. The average inter-vehicle distance deviations of different approaches only have a slight difference and maintain within a small value, with the average distance deviation smaller than 1.5 m. To sum up, the proposed method can maintain acceptable performance in both fuel economy and driving safety with the impact of information deviation.

TABLE V
SIMULATION RESULTS WITH DIFFERENT DEVIATIONS IN THE COOPERATIVE INFORMATION

Method	Powertrain energy consumption cost (CNY)	Reduction (%)	Deviations in cooperative information (m)	Average inter-vehicle distance deviation (m)
PID-ACC	1.69	-	-	1.44
C-EACC in deal condition	1.55	8.28	0	1.44
C-EACC with information deviation case I	1.61	4.73	1.01	1.42
C-EACC with information deviation case II	1.62	4.14	1.16	1.42
C-EACC with information deviation case III	1.64	2.96	1.55	1.42

To further validate the adaptability of C-EACC to different driving cycles, a real-world driving cycle, which was collected in Chongqing, China, is exploited to examine the performance of the proposed method as well. The initial inter-vehicle distance and initial SOC are defined as 15 m and 0.38, respectively. The results of velocity optimization are shown in Fig. 11. It can be observed that the C-EACC method can precisely track the preceding vehicle velocity, and the velocity waves of the host vehicle are significantly restrained, compared with the PID-ACC method and the ADP-ACC method. Additionally, the inter-vehicle distance with the C-EACC method is kept within the safe range, which indicates that driving safety is fulfilled as well. Simulation results verify that the prosed method shows satisfactory performance in speed tracking capability and driving safety under real driving cycles.

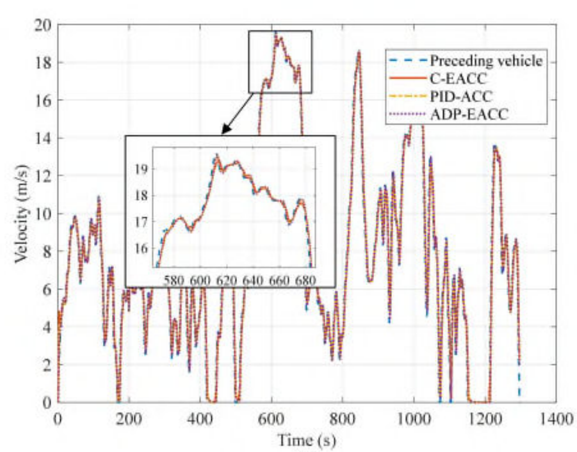

(a)

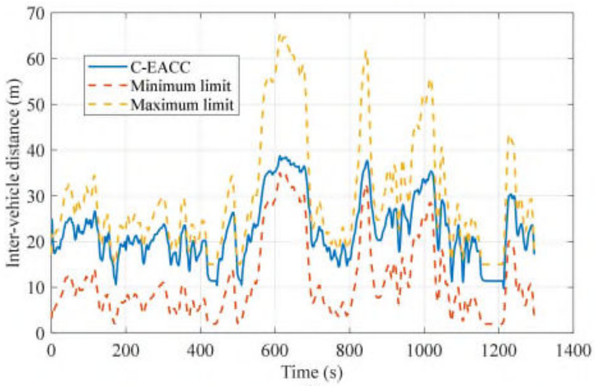

(b)

Fig. 11. Simulation results of the real-world driving cycle. (a) velocity profiles, (b) inter-vehicle distance.

To quantitatively evaluate the performance of proposed method, the simulation results of three methods with different initial SOC are summarized in Table VI. Compared with the PID-ACC method, the proposed C-EACC method remarkably promotes the fuel economy under different initial SOC, with the increase of up to 8.74%. While, the ADP-EACC method leads to slight fuel economy improvement of up to 1.94%. These results showcase similar trend with the simulation in UDDS driving cycle. Besides, it can be found that the fuel economy improvement is increased with the increase of electricity power, except for the case with initial SOC of 0.4. The reason is that this case has sufficient electricity power and the host vehicle drives in electric mode during the whole driving cycle, i.e., drives similar to EVs. This phenomenon also manifests that velocity optimization plays a significant role in fuel economy improvement for PHEVs. In summary, the simulation results validate that the proposed method shows strong adaptivity to cooperative information deviations and different driving cycles, and the fuel economy of PHEV is notably improved with the incorporation of cooperative information.

TABLE VI
SIMULATION RESULTS OF THE PROPOSED METHOD WITH REAL-WORLD DRIVING CYCLE

Initial SOC	C-EACC		ADP-EACC		PID-ACC
	Energy consumption cost (CNY)	Fuel economy improvement (%)	Energy consumption cost (CNY)	Fuel economy improvement (%)	Energy consumption cost (CNY)
0.4	0.60	3.23	0.61	1.61%	0.62
0.38	0.94	8.74	1.01	1.94%	1.03
0.34	1.93	2.53	1.96	1.01%	1.98
0.31	2.73	1.80	2.77	0.36%	2.78

V. CONCLUSION

In this study, a cooperative Eco-ACC approach is proposed to improve fuel economy for PHEVs under car-following scenarios. The constructed controller is model-free and enables to forwardly search the optimal control decisions efficiently without establishing explicit numerical modeling. An actor-critic structure is designed to construct an ADP-based car-following controller, thereby achieving adaptively real-time control. Furthermore, a data-driven energy consumption model is leveraged to generate reinforcement signal which sufficiently integrates nonlinear characteristics of the hybrid powertrain system. To dampen unnecessary velocity fluctuations of the host vehicle and further reduce energy consumption, the cooperative information from the preceding vehicle transferred via V2V communication is exploited to regulate the input of the proposed controller. The simulation results demonstrate that the proposed method can obviously reduce energy consumption by up to 8.28% and 8.74% for UDDS and real-world driving cycles in comparison with the traditional methods. Moreover, the proposed method also effectively reduces energy consumption with the influence of cooperative information deviations and different driving conditions, showing preferable performance in adaptability.

Our future work will be focused on developing eco-driving control in a complex driving environment based on an efficient learning-based method. The environment information, including traffic lights, speed limits, and road conditions, etc., will be taken into consideration in our future study. In addition, experiment platform, including hardware-in-loop platform or real vehicle, will be established to validate the proposed eco-driving control methods.

REFERENCES

[1] M. Contestabile, M. Alajaji, and B. Almubarak, "Will current electric vehicle policy lead to cost-effective electrification of passenger car transport?," *Energy Policy,* vol. 110, pp. 20-30, 2017.

[2] Z. Li, A. Khajepour, and J. Song, "A comprehensive review of the key technologies for pure electric vehicles," *Energy,* vol. 182, pp. 824-839, 2019.

[3] Z. Chen, Y. Liu, M. Ye, Y. Zhang, and G. Li, "A survey on key techniques and development perspectives of equivalent consumption minimisation strategy for hybrid electric vehicles," *Renewable and Sustainable Energy Reviews,* vol. 151, p. 111607, 2021.

[4] T. Liu, W. Tan, X. Tang, J. Zhang, Y. Xing, and D. Cao, "Driving conditions-driven energy management strategies for hybrid electric vehicles: A review," *Renewable and Sustainable Energy Reviews,* vol. 151, p. 111521, 2021.

[5] M. Montazeri, A. Fotouhi, and A. Naderpour, "Driving segment simulation for determination of the most effective driving features for HEV intelligent control," *Vehicle system dynamics,* vol. 50, no. 2, pp. 229-246, 2012.

[6] A. Stippich *et al.*, "Key components of modular propulsion systems for next generation electric vehicles," *CPSS Transactions on Power Electronics and Applications,* vol. 2, no. 4, pp. 249-258, 2017.

[7] Z. Wang, G. Wu, and M. J. Barth, "Cooperative Eco-Driving at Signalized Intersections in a Partially Connected and Automated Vehicle Environment," *IEEE Transactions on Intelligent Transportation Systems,* Article vol. 21, no. 5, pp. 2029-2038, 2020, Art no. 8704319.

[8] U. Montanaro *et al.*, "Towards connected autonomous driving: review of use-cases," *Vehicle system dynamics,* vol. 57, no. 6, pp. 779-814, 2019.

[9] H. Yang, F. Almutairi, and H. Rakha, "Eco-driving at signalized intersections: A multiple signal optimization approach," *IEEE Transactions on Intelligent Transportation Systems,* vol. 22, no. 5, pp. 2943-2955, 2020.

[10] Y. Liu, Z. Huang, J. Li, M. Ye, Y. Zhang, and Z. Chen, "Cooperative optimization of velocity planning and energy management for connected plug-in hybrid electric vehicles," *Applied Mathematical Modelling,* vol. 95, pp. 715-733, 2021.

[11] F. Zhang, X. Hu, R. Langari, and D. Cao, "Energy management strategies of connected HEVs and PHEVs: Recent progress and outlook," *Progress in Energy and Combustion Science,* vol. 73, pp. 235-256, 2019.

[12] S. Xu, S. E. Li, H. Peng, B. Cheng, X. Zhang, and Z. Pan, "Fuel-saving cruising strategies for parallel HEVs," *IEEE Transactions on Vehicular Technology,* Article vol. 65, no. 6, pp. 4676-4686, 2016, Art no. 7296694.

[13] Z. Ye, K. Li, M. Stapelbroek, R. Savelsberg, M. Gunther, and S. Pischinger, "Variable Step-Size Discrete Dynamic Programming for Vehicle Speed Trajectory Optimization," *IEEE Transactions on Intelligent Transportation Systems,* Article vol. 20, no. 2, pp. 476-484, 2019, Art no. 8320319.

[14] D. Shen, D. Karbowski, and A. Rousseau, "Fuel-Optimal Periodic Control of Passenger Cars in Cruise Based on Pontryagin's Minimum Principle," *IFAC-PapersOnLine,* Article vol. 51, no. 31, pp. 813-820, 2018.

[15] J. Li, Y. Liu, Y. Zhang, Z. Lei, Z. Chen, and G. Li, "Data-driven based eco-driving control for plug-in hybrid electric vehicles," *Journal of Power Sources,* vol. 498, p. 229916, 2021.

[16] Q. Guo, O. Angah, Z. Liu, and X. J. Ban, "Hybrid deep reinforcement learning based eco-driving for low-level connected and automated vehicles along signalized corridors," *Transportation Research Part C: Emerging Technologies,* vol. 124, p. 102980, 2021.

[17] C. Sun, J. Guanetti, F. Borrelli, and S. J. Moura, "Optimal Eco-Driving Control of Connected and Autonomous Vehicles Through Signalized Intersections," *IEEE Internet of Things Journal,* Article vol. 7, no. 5, pp. 3759-3773, 2020, Art no. 8964352.

[18] C. Sun, C. Zhang, H. Yu, W. Liang, Q. Ren, and J. Li, "An Eco-driving Approach with Flow Uncertainty Tolerance for Connected Vehicles against Waiting Queue Dynamics on Arterial Roads," *IEEE Transactions on Industrial Informatics,* 2021.

[19] J. Zhou and H. Peng, "Range policy of adaptive cruise control vehicles for improved flow stability and string stability," *IEEE Transactions on intelligent transportation systems,* vol. 6, no. 2, pp. 229-237, 2005.

[20] H. Liu, C. Miao, and G. G. Zhu, "Economic adaptive cruise control for a power split hybrid electric vehicle," *IEEE Transactions on Intelligent Transportation Systems,* vol. 21, no. 10, pp. 4161-4170, 2019.

[21] S. Xie, X. Hu, T. Liu, S. Qi, K. Lang, and H. Li, "Predictive vehicle-following power management for plug-in hybrid electric vehicles," *Energy,* vol. 166, pp. 701-714, 2019.

[22] L. Xie, Y. Luo, D. Zhang, R. Chen, and K. Li, "Intelligent energy-saving control strategy for electric vehicle based on preceding vehicle movement," *Mechanical Systems and Signal Processing,* vol. 130, pp. 484-501, 2019.

[23] B. Chen, S. A. Evangelou, and R. Lot, "Series Hybrid Electric Vehicle Simultaneous Energy Management and Driving Speed Optimization," *IEEE/ASME Transactions on Mechatronics,* vol. 24, no. 6, pp. 2756-2767, 2020.

[24] F. Morlock and O. Sawodny, "An economic model predictive cruise controller for electric vehicles using gaussian process prediction," *IFAC-PapersOnLine,* vol. 51, no. 31, pp. 876-881, 2018.

[25] S. Zhang, Y. Luo, J. Wang, X. Wang, and K. Li, "Predictive energy management strategy for fully electric vehicles based on preceding vehicle movement," *IEEE Transactions on Intelligent Transportation Systems,* vol. 18, no. 11, pp. 3049-3060, 2017.

[26] G. Li and D. Görges, "Ecological adaptive cruise control and energy management strategy for hybrid electric vehicles based on heuristic dynamic programming," *IEEE Transactions on Intelligent Transportation Systems,* vol. 20, no. 9, pp. 3526-3535, 2018.

[27] G. Li and D. Görges, "Ecological Adaptive Cruise Control for Vehicles With Step-Gear Transmission Based on Reinforcement Learning," *IEEE Transactions on Intelligent Transportation Systems,* 2019.

[28] X. Qu, Y. Yu, M. Zhou, C.-T. Lin, and X. Wang, "Jointly dampening traffic oscillations and improving energy consumption with electric, connected and automated vehicles: a reinforcement learning based approach," *Applied Energy,* vol. 257, p. 114030, 2020.

[29] Y. Shao and Z. Sun, "Eco-approach with traffic prediction and experimental validation for connected and autonomous vehicles," *IEEE Transactions on Intelligent Transportation Systems,* vol. 22, no. 3, pp. 1562-1572, 2020.

[30] Y. Bian, Y. Zheng, W. Ren, S. E. Li, J. Wang, and K. Li, "Reducing time headway for platooning of connected vehicles via V2V communication," *Transportation Research Part C: Emerging Technologies,* vol. 102, pp. 87-105, 2019.

[31] F. Ma *et al.*, "Predictive energy-saving optimization based on nonlinear model predictive control for cooperative connected vehicles platoon with V2V communication," *Energy,* vol. 189, p. 116120, 2019.
[32] L. Xiao and F. Gao, "Practical string stability of platoon of adaptive cruise control vehicles," *IEEE Transactions on intelligent transportation systems,* vol. 12, no. 4, pp. 1184-1194, 2011.
[33] V. Milanés, S. E. Shladover, J. Spring, C. Nowakowski, H. Kawazoe, and M. Nakamura, "Cooperative adaptive cruise control in real traffic situations," *IEEE Transactions on intelligent transportation systems,* vol. 15, no. 1, pp. 296-305, 2013.
[34] A. Vahidi and A. Sciarretta, "Energy saving potentials of connected and automated vehicles," *Transportation Research Part C: Emerging Technologies,* vol. 95, pp. 822-843, 2018.
[35] S. Zhang, Y. Luo, K. Li, and V. Li, "Real-time energy-efficient control for fully electric vehicles based on an explicit model predictive control method," *IEEE Transactions on Vehicular Technology,* vol. 67, no. 6, pp. 4693-4701, 2018.
[36] J. Han, A. Sciarretta, L. L. Ojeda, G. De Nunzio, and L. Thibault, "Safe-and eco-driving control for connected and automated electric vehicles using analytical state-constrained optimal solution," *IEEE Transactions on Intelligent Vehicles,* vol. 3, no. 2, pp. 163-172, 2018.
[37] Y. Kim, M. Figueroa-Santos, N. Prakash, S. Baek, J. B. Siegel, and D. M. Rizzo, "Co-optimization of speed trajectory and power management for a fuel-cell/battery electric vehicle," *Applied Energy,* vol. 260, p. 114254, 2020.
[38] F. Ma *et al.*, "Eco-driving-based cooperative adaptive cruise control of connected vehicles platoon at signalized intersections," *Transportation Research Part D: Transport and Environment,* vol. 92, p. 102746, 2021.
[39] M. Vajedi and N. L. Azad, "Ecological adaptive cruise controller for plug-in hybrid electric vehicles using nonlinear model predictive control," *IEEE Transactions on Intelligent Transportation Systems,* vol. 17, no. 1, pp. 113-122, 2015.
[40] H. Liu, X.-Y. Lu, and S. E. Shladover, "Traffic signal control by leveraging Cooperative Adaptive Cruise Control (CACC) vehicle platooning capabilities," *Transportation research part C: emerging technologies,* vol. 104, pp. 390-407, 2019.
[41] S. Halbach, P. Sharer, S. Pagerit, A. Rousseau, and C. Folkerts, "Model architecture, methods, and interfaces for efficient math-based design and simulation of automotive control systems," *SAE Technical Paper,* vol. 20100241, 2010.
[42] L. Liang, X. Wang, and S. Jian, "Fuel consumption optimization for smart hybrid electric vehicle during a car-following process," *Mechanical Systems & Signal Processing,* vol. 87, no. 1, pp. 17-29, 2017.
[43] R. Song, Q. Wei, and Q. Li, *Adaptive dynamic programming: single and multiple controllers.* Springer, 2019.
[44] J. Li, X. Wu, S. Hu, and J. Fan, "A Deep Reinforcement Learning Based Energy Management Strategy for Hybrid Electric Vehicles in Connected Traffic Environment," *IFAC-PapersOnLine,* vol. 54, no. 10, pp. 150-156, 2021.

Jie Li received the B.S and M.S in mechanical engineering and automotive engineering from Chongqing University, Chongqing, China, in 2015 and 2018, respectively. From 2018 to 2019, he was a Research Engineer with Guangzhou Automobile Group, Guangzhou, China. He is currently working toward the Ph.D. degree with Chongqing University, Chongqing, China. He is also a joint Ph.D. student with Cranfield University, UK, from 2021 to 2022. His research interests include eco-driving control of the connected and automated vehicles, optimal control and energy management of hybrid electric vehicles

Yonggang Liu (Senior Member, IEEE) received the B.S and Ph.D. in automotive engineering from Chongqing University, Chongqing, China, in 2004 and 2010, respectively. He was a joint Ph.D. student and a research scholar at University of Michigan-Dearborn, MI, USA, from 2007 to 2009.

Now he is a Professor with College of Mechanical and Vehicle Engineering at Chongqing University. He is also a committee member of vehicle control and intelligence society of Chinese Association of Automation (CAA). His research interests mainly include optimization and control of intelligent electric and hybrid vehicles and integrated control of vehicle automatic transmission system. He has leaded more than 20 research projects, such as the National Natural Science Foundation of China (both Youth Fund and General Program), Ph.D. Programs Foundation of Ministry of Education of China. He has published more than 90 research journal papers.

Abbas Fotouhi (M'13–SM'21) received his PhD degree in mechanical engineering from Iran University of Science and Technology in 2011. He is currently a Senior Lecturer in Advanced Vehicle Engineering Centre at Cranfield University. Before joining Cranfield in 2014, he was with the Centre for Artificial Intelligence and Robotics (CAIRO) at University Technology Malaysia. Dr Fotouhi's expertise are dynamical systems modelling, simulation, optimization, and control. In addition, he has extensive practical and algorithmic experience of applying AI and Machine Learning techniques in engineering problems. His current research includes electrified vehicle powertrain systems, batteries, and transportation system optimization. Dr Fotouhi is a fellow of the UK Higher Education Academy and fellow of the Faraday Institution in UK.

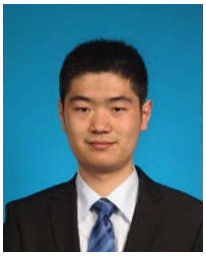

Xiangyu Wang received the B.S. and Ph.D. from Tsinghua University, Beijing, China, in 2015 and 2020, where he is currently working as assistant professor in mechanical engineering at the School of Vehicle and Mobility, Tsinghua University.

His research interests include intelligent hybrid electric vehicle powertrain design and control.

Zheng Chen (Senior Member, IEEE) received the B.S. and M.S. in electrical engineering and the Ph.D. in control science engineering from Northwestern Polytechnical University, Xi'an, China, in 2004, 2007, and 2012, respectively.

He is currently a Professor of Faculty of Transportation Engineering at Kunming University of Science and Technology, Kunming, Yunnan, China. He was a Postdoctoral Fellow and a Research Scholar with the University of Michigan, Dearborn, USA from 2008 to 2014. His research interests include battery management system, battery status estimation, and energy management of hybrid electric vehicles. He has conducted more than 20 projects and has published more than 80 peer-reviewed journal papers and conference proceedings. He is the receiver of Yunnan Oversea High Talent Project, China and the second place of IEEE VTS Motor Vehicles Challenge in 2017 and 2018.

Yuanjian Zhang (Member, IEEE) received the M.S. degree in automotive engineering from the Coventry University, Coventry, U.K., in 2013, and the Ph.D. degree in automotive engineering from Jilin University, Changchun, China, in 2018. Then, he joined the University of Surrey, Guildford, U.K., as a Research Fellow in advanced vehicle control. In early 2019, he secured a Research Fellow position with Sir William Wright Technology Centre, Queen's University Belfast, Belfast, U.K. He is currently a Lecturer (Assistant Professor) with the Department of Aeronautical and Automotive Engineering, Loughborough University, Loughborough, U.K. He has authored several books and more than 50 peer-reviewed journal papers and conference proceedings. His current research interests include advanced control on electric vehicle powertrains, vehicle-environment-driver cooperative control, vehicle dynamic control, and intelligent control for driving assist system.

Liang Li (M'15–SM'17) received the Ph.D. degree from the Department of Automotive Engineering, Tsinghua University, Beijing, China, in 2008. Since 2011, he has been an Associate Professor with Tsinghua University. From November 2011 to December 2012, he was a Researcher with the Institute for Automobile Engineering, RWTH Aachen University, Aachen, Germany. Dr. Li was the recipient of the China Automotive Industry Science and Technology Progress Award for his achievements in hybrid electrical bus, in 2012, and the National Science Fund for Excellent Young Scholars of the People's Republic of China, in 2014.

His research interests mainly include vehicle dynamics and control, adaptive and nonlinear system control, and hybrid vehicle develop and control.